Original Article

Role of reactive oxygen species in high concentration glucose-induced growth inhibition of human peritoneal mesothelial cells

Nan Zhu[1]^, Yunhai Tang[2], Weijie Yuan[1], Zhihuan Tang[1,2]

[1]Department of Nephrology, Shanghai General Hospital, Shanghai Jiao Tong University School of Medicine, Shanghai, China; [2]Department of Nephrology, Jiading Branch of Shanghai General Hospital, Shanghai, China

Contributions: (I) Conception and design: Z Tang, N Zhu; (II) Administrative support: W Yuan; (III) Provision of study materials or patients: Y Tang; (IV) Collection and assembly of data: N Zhu; (V) Data analysis and interpretation: Z Tang, N Zhu; (VI) Manuscript writing: All authors; (VII) Final approval of manuscript: All authors.

Correspondence to: Zhihuan Tang. Department of Nephrology, Shanghai General Hospital, Shanghai Jiao Tong University School of Medicine, No. 100 Haining Road, Shanghai 200080, China. Email: xiaotang1516@gmail.com.

Background: To investigate the effects and mechanism of high concentration glucose (HG), exogenous hydrogen peroxide (H_2O_2), and antioxidants on the cell growth (cell proliferation) of human peritoneal mesothelial cells (HPMCs).

Methods: All tests were conducted on cultured HPMCs (HMrSV5) *in vitro*. Various concentrations of glucose (0.1%, 1.35%, and 3.86%), H_2O_2 (0.5 and 0.1 mmol/L), and antioxidants (pyruvate and catalase) were used in cell culture. Moreover, in order to study the interaction between these factors, HG and H_2O_2, HG and antioxidants, HG, H_2O_2, and antioxidants, were used respectively. After 12–24 h, phase-contrast microscopy was used to examine the morphological changes of HPMCs. DNA synthesis was detected by ^{3}H-thymidine incorporation to measure cell proliferation, and flow cytometry was used to evaluate the proportion of cells in G_1 phase. Furthermore, semiquantitative reverse-transcription polymerase chain reaction (RT-PCR) was utilized to determine the mRNA expression of $p21^{Waf1}$ and $p27^{Kip1}$ [cyclin-dependent kinase inhibitors (CKIs)], while immunocytochemistry (ICC) and Western blotting were employed to measure the protein expression of $p21^{Waf1}$ and $p27^{Kip1}$.

Results: HG or low-dose exogenous H_2O_2 resulted in hypertrophy and senescence of HPMCs, resulting in similar morphological changes. Both HG and exogenous H_2O_2 (0.5 mmol/L) inhibited the proliferation of HPMCs and led to G1 phase arrest of HPMCs. The proportion of cells in G_1 phase increased. Moreover, HG enhanced the toxic effects of exogenous H_2O_2. Both HG and exogenous H_2O_2 increased the expression of $p21^{Waf1}$ and $p27^{Kip1}$. The addition of an antioxidant in HG medium arrested cells in the G_1 phase and improved the inhibited cell proliferation.

Conclusions: Both HG and exogenous H_2O_2 treatments can induce growth inhibition of HPMCs by arresting cell cycle progression, which is partially due to the increased expression of $p21^{Waf1}$ and $p27^{Kip1}$. Thus, the effects of HG might be associated with endogenous reactive oxygen species (ROS), and it might be beneficial to use antioxidants in peritoneal dialysis (PD).

Keywords: Human peritoneal mesothelial cells (HPMCs); cell proliferation; reactive oxygen species (ROS); glucose

Submitted Jul 25, 2022. Accepted for publication Sep 26, 2022.
doi: 10.21037/atm-22-4352
View this article at: https://dx.doi.org/10.21037/atm-22-4352

^ ORCID: 0000-0003-4710-4571.

Introduction

Peritoneal dialysis (PD) is an effective life-sustaining treatment for patients with end-stage renal disease. The peritoneum may become dysfunctional as a dialysis organ over time because of progressive membrane injury. As a result of prolonged exposure to bioincompatible PD fluid (PDF) that contains high levels of glucose and degradation products of glucose, low pH, and high osmolality, peritonitis develops (1). Human peritoneal mesothelial cells (HPMCs) play an important role in peritoneal membrane injury (2). Hypertrophy and arrest of the cell cycle induced by high concentration glucose (HG) in renal mesangial cells in the early stage of diabetic nephropathy, which might be one of the factors of the initiation or progression of the disease (3). A recent study demonstrated that HG inhibits the growth of HPMCs (4). Another study showed that HG causes hypertrophy, senescence, cell cycle arrest, apoptosis, and necrosis, epithelial-to-mesenchymal transition (EMT), peritoneal angiogenesis, which are detrimental to continuous ambulatory PD (CAPD) patients (5,6). Regarding the mechanism of HG cytotoxicity, the oxidative stress state induced by reactive oxygen species (ROS) has been the subject of increasing interest for CAPD patients (7). There is not only increased generation of ROS by mesothelial cells but also by peritoneal phagocytes. ROS can damage HPMCs, but the mechanism of damage remains unclear. ROS can inhibit cell growth and induce cell cycle arrest in other types of cells, such as mesangial and proximal tubular cells (3). Belonging to the *CIP/KIP* family of cyclin-dependent kinase inhibitors (CKIs), $p21^{Waf1}$ and $p27^{kip1}$ are negative regulators of the cell cycle. Some effects of HG have been associated with increased expression of $p21^{Waf1}$ (8). Additionally, mammalian cells produce hydrogen peroxide (H_2O_2), in low concentrations, H_2O_2 plays an important role in cell proliferation, immunity, and metabolism. However, higher non-physiologic concentrations of H_2O_2 can cause oxidative stress. Stress can lead to cell death if it is not alleviated (9). H_2O_2 is involved in various processes including inducing hypertrophic and senescent phenotypes in some cell types, arresting the cell cycle, and increasing the expression of $p21^{Waf1}$ and $p27^{Kip1}$ (10-12). Presently, there is no report on the reciprocal effects of these factors and the role of ROS in HG-induced changes in the cell cycle and growth of HPMCs. Therefore, we designed this preliminary study to explore these correlations. We present the following article in accordance with the MDAR reporting checklist (available at https://atm.amegroups.com/article/view/10.21037/atm-22-4352/rc).

Methods

Cell culture

A HPMC line, HMrSV5 (kindly provided by Prof. Pierre Ronco, Hospital Tenon, Paris, France), was cultured in Dulbecco's modified Eagle's medium (DMEM; Gibco, NY, USA) supplemented with 10% fetal calf serum (FCS; Gibco, NY, USA), 20 mmol/L hydroxyethyl piperazine ethane sulfonic acid (HEPES; Gibco, NY, USA), and 2 mmol/L L-glutamine at 37 ℃ in a humidified atmosphere with 5% CO_2.

Research design

The study was divided into 2 parts—part A and part B—to observe the effects of HG and H_2O_2 purchased from Nanjing Chemical Reagent (Nanjing, China) on HPMCs, respectively. All the test solutions used DMEM for all stimulations.

Part A comprised 8 groups: group a1 with 0.1% glucose in DMEM (G_0) as the control group, group a2 with 1.35% glucose (1.35G), group a3 with 3.86% glucose (3.86G), group a4 with 3.86% mannitol (MCE, Shanghai, China) (3.86M), group a5 with pyruvate 35 mmol/L in DMEM (G_0 + P), group a6 with 3.86% glucose and pyruvate (MCE) 35 mmol/L (3.86G + P), group a7 with catalase 500 U/L (G_0 + C), and group a8 with 3.86% glucose and catalase 500 U/L in DMEM (3.86G + C). Part B consisted of 6 groups: group b1 with H_2O_2 0.5 mmol/L in DMEM (G_0 + 0.5H), group b2 with H_2O_2 0.1 mmol/L (G_0 + 0.1H), group b3 with H_2O_2 0.5 mmol/L and 3.86% glucose (3.86G + 0.5H), group b4 with H_2O_2 0.1 mmol/L and 3.86% glucose (3.86G + 0.1H), group b5 with H_2O_2 0.5 mmol/L, 3.86% glucose, and pyruvate 35 mmol/L (3.86G + 0.5H + P), group b6 with 0.1% glucose (G_0, control group). Unless noted otherwise, the stimulation time was 24 and 12 h in part A and B, respectively. Each experiment was performed with 3 independent replicates.

Morphological observation

The HPMCs were harvested from culture flasks by trypsin digestion and centrifugation as described previously, and inoculated into a 24-well culture plate at 6.0×10^4 cells/well and grown at 37 ℃ in a 5% CO_2 incubator. When the cells reached to logarithmic phase, incubated with 0.1% glucose, 3.86% glucose, and 0.5 mmol/L H_2O_2. Then, the morphological changes were observed under a phase-contrast microscope 24 h post-stimulation.

Flow cytometric analysis

Cells of groups a1–a6 and b1–b6 were assessed by flow cytometry 12–24 h post-incubation. Subsequently, the cells were washed with phosphate-buffered saline (PBS), trypsinized, fixed with 70% ethanol at 4 ℃ overnight, and stained with propidium iodide (PI) for 30 min. Then, 10^6 cells/mL in each group were harvested and analyzed on a FACS Epics XL Flow Cytometer (Coulter) to elucidate cell cycle distribution and calculate the proportion of cells in the G_1 phase.

Cell proliferation studies with 3H-thymidine incorporation

The proliferation of the HPMCs was estimated indirectly based on the incorporation of ^{3}H-thymidine into growing cells that were seeded in a 96-well plate at a density of 10^3 cells/well. After 48 h, the cells were exposed to the test solutions (groups a1–a8 and b1–b6, i.e., 14 groups) for 24 h. Subsequently, ^{3}H-thymidine (1 Ci/well, procured from Chinese Science Academy, Shanghai Institute of Nuclear Research) was added for an additional 6-h incubation period. Then, the test solutions were discharged, and the cells were trypsinized and collected on a filter paper using a semi-automatic cell collector (type of DYQIII). The filter papers were placed into the tube, and the scintillation reagent was added to count the samples in a beta counter (Pharmacia).

Reverse-transcription polymerase chain reaction (RT-PCR)

Total RNA was extracted from HPMCs in the a1–a6 and b1–b6 groups using TRIzol as stated by the protocol. An equivalent of 2 μg of RNA was reversed transcribed into complementary DNA (cDNA) using M-MLV reverse transcriptase (Gibco, NY, USA). PCR amplification was performed in a total volume of 50 μL using the following protocol: 94 ℃ for 5 min, 25 cycles of 94 ℃ for 1 min, 65 ℃ (*p21*) for 30 s, 58 ℃ (*GAPDH*) for 30 s, 72 ℃ for 1 min, and finally, 72 ℃ for 7 min. The PCR products were separated by 2% agarose gel electrophoresis with 0.5 μg/mL ethidium bromide and photographed. Bands were scanned using a densitometer (Gensnap), and band density was compared to that of the housekeeping gene. The sequences of the amplification primers were as follows: $p21^{Waf1}$ (sense: 5'-CAGGGGACAGCAGAGGAAGA-3', antisense 5'-GGGCGGCCAGGGTATGTAC-3'), $p27^{Kip1}$ (sense: 5'-ATGTCAAACGTGCGAGTGTC-3', antisense: 5'-TCTGTAGTAGAACTCGGGCAA-3'), *GAPDH* (sense: 5'-CCACCCATGGCAAATTCCATGGCA-3', antisense: 5'-TCTAGAGGGCAGGTCAGGTCCACC-3').

Immunocytochemistry (ICC)

HPMCs were grown on 1×1 cm^2 slides and stimulated with various test solutions (groups a1–a8 and b1–b6) for 12–24 h. Then, the stimulations were removed, and the cell layer was rinsed with PBS. Subsequently, the cells were fixed with freshly prepared 4% paraformaldehyde at room temperature for 20 min. Then, the cells were rehydrated with PBS and incubated with a primary antibody (mouse anti-human $p21^{Waf1}$ or rabbit anti-human $p27^{Kip1}$) for 4 ℃ overnight (1:100 dilution, Santa Cruz, CA, USA). After washing with PBS, the cells were incubated with horseradish peroxidase (HRP)-conjugated secondary antibody (37 ℃ for 2 h), and the immune reaction was detected by 3,3'-diaminobenzidine (DAB). The nuclei were counterstained with hematine. Computer software was used for semiquantitative analysis to calculate the proportion of positive cells.

Western blot

Groups a1, a3, a6, and b3 were stimulated in a 90-mm dish for 24 h. Then total cellular proteins extracted from the HPMCs, quantified, separated by sodium dodecyl sulfate (SDS)-polyacrylamide gel electrophoresis (PAGE). After electrophoresis and transfer (nitrocellulose membrane, Bio-Rad, Amresco), the polyvinylidene fluoride (PVDF) membranes were blocked in 5% milk prior and probed with mouse monoclonal antibody to human $p21^{Waf1}$ and rabbit anti-human $p27^{Kip1}$ (Santa Cruz, CA, USA). This was followed by incubation with the secondary antibody, namely HRP-conjugated goat anti-mouse IgG (Yeasen, Shanghai, China). Finally, the membranes were developed using enhanced chemiluminescence (ECL) blotting substrate (Amersham, USA) and exposed to X-ray film. Glyceraldehyde 3-phosphate dehydrogenase (GAPDH) was used as a control. The immunoreactive band intensity was measured on an image analysis system (Genesnap).

Statistical analysis

Data are shown as the mean ± standard error of the mean (SEM). Each experiment was repeated at least 3 times. Student's *t*-test or one-way analysis of variance (ANOVA) were used for statistical analysis using SPSS 10 software

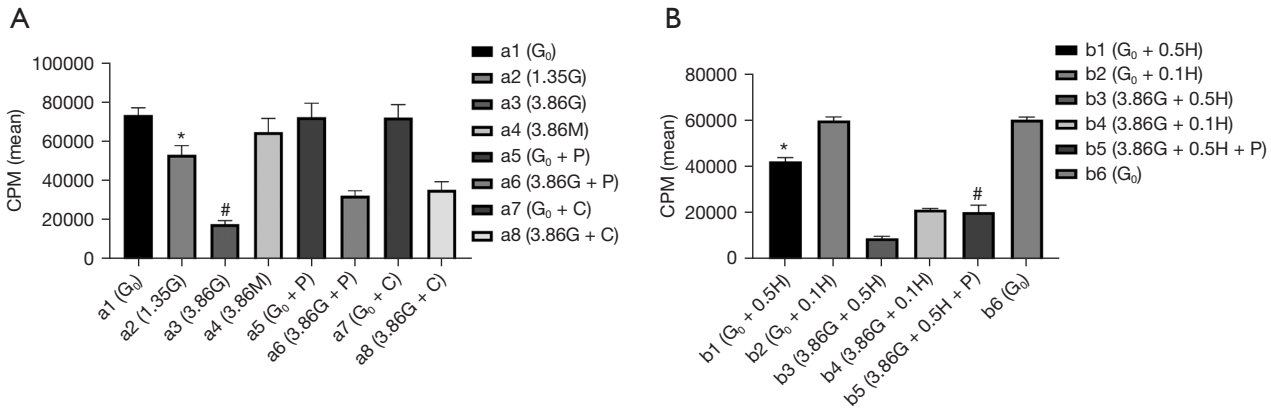

Figure 1 ^{3}H-thymidine incorporation analysis. (A) Effect of glucose and antioxidants on HPMCs proliferation. *, a2 *vs.* a1, a2 *vs.* a3, P<0.05; #, a3 *vs.* a5, a3 *vs.* a7, P<0.05. a1: with 0.1% glucose in DMEM (G_0), as the control group; a2: with 1.35% glucose (1.35G); a3: with 3.86% glucose (3.86G); a4: with 3.86% mannitol (3.86M); a5: with pyruvate 35 mmol/L in DMEM (G_0 + P); a6: with 3.86% glucose and pyruvate 35 mmol/L (3.86G + P); a7: with catalase 500 U/L (G_0 + C); a8: with 3.86% glucose and catalase 500 U/L in DMEM (3.86G + C). (B) Effect of glucose, H_2O_2, and the antioxidant on the proliferation of HPMCs. *, b1 *vs.* b6, b1 *vs.* b3, P<0.05; #, b5 *vs.* b3, P<0.05. b1: with H_2O_2 0.5 mmol/L in DMEM (G_0 + 0.5H); b2: with H_2O_2 0.1 mmol/L (G_0 + 0.1H); b3: with H_2O_2 0.5 mmol/L and 3.86% glucose (3.86G + 0.5H); b4: with H_2O_2 0.1 mmol/L and 3.86% glucose (3.86G + 0.1H); b5: with H_2O_2 0.5 mmol/L, 3.86% glucose, and pyruvate 35 mmol/L (3.86G + 0.5H + P); b6: with 0.1% glucose (G_0), as the control group. CPM, count per minute; HPMC, human peritoneal mesothelial cell; DMEM, Dulbecco's modified Eagle's medium; H_2O_2, hydrogen peroxide.

(IBM Corporation, Armonk, NY, USA). P<0.05 was considered statistically significant.

Results

Morphological observations

Morphological changes were observed after 24-h stimulation. The HPMCs in group G_0 (control group) showed a typical polygonal and cobblestone monolayer appearance when grown to confluency. In the 3.86G group, the nucleolus was obvious, with the appearance of poly-nuclei and hypertrophy of the cell. In the 0.5 mmol/L H_2O_2 group, the changes were similar to that in the HG group.

Effects of various stimulations on cell growth (proliferation)

No significant difference in cell growth was observed among group a1 (G_0), a5 (G_0 + P), and a7 (G_0 + C), and the count per minute (CPM) was higher than that in group a2 (1.35G) or a3 (3.86G). No difference was detected between the cell numbers in group a6 (3.86G + P) and a8 (3.86G + C), but both had significantly higher cell numbers than group a3 (*Figure 1A*).

A high concentration of H_2O_2 (0.5 mmol/L) inhibited the proliferation of HPMCs, which was not demonstrated with the 0.1 mmol/L dose (b2 *vs.* b6, P>0.05). This effect was accentuated by HG conditions (b1 *vs.* b3, P<0.05), while antioxidant treatment attenuated this effect (b3 *vs.* b5, P<0.05) (*Figure 1B*).

Effects of various stimulations on the cell cycle

HG conditions elevated the proportion of G_1 phase cells (shown as percent in parentheses) in a dose-dependent manner. Compared to the a2 (77.1±7.40) or a3 (82.3±6.20) groups, the a1 group (68.2±42.5) (control) differed significantly (P<0.05). However, no significant difference was detected between the proportion in high osmolality a4 (70.1±5.21) and a1 (control) (P>0.05). Without HG, pyruvate did not change the proportion of G1 phase significantly [a5 (72.2±6.22) *vs.* a1] (P>0.05). After adding the antioxidant, the proportion in the a6 group (72.2±5.32) was decreased compared to the a3 group (82.3±6.20) (P<0.05).

Moreover, the proportion of G_1 phase cells was increased, and HG enhanced this effect [comparing group b1 (75.2±5.35) with b6 (65.3±7.21), b3 (86.2±7.10) with b1, and b4 (80.2±8.12) with b2 (71.1±4.02), P<0.05]. However,

after adding the antioxidants, the proportion was decreased when comparing the b5 group (72.2±4.22) to the b3 group (P<0.05).

Effects of various stimulations on $p21^{Waf1}$ expression

The expression of $p21^{Waf1}$ mRNA in group a3 was maximal. Following stimulation of HPMCs with HG and H_2O_2 (*Figure 2A-2D*), $p21^{Waf1}$ mRNA expression was elevated compared with the control in a dose-dependent manner (a3 *vs.* a2, a2 *vs.* a1; b2 *vs.* b6, P<0.05). After adding the antioxidant in the HG- (a3 *vs.* a6) or H_2O_2-containing medium (b3 *vs.* b5), the expression was significantly reduced in both. Moreover, no statistically significant difference was detected in $p21^{Waf1}$ gene expression among groups a4, a5, and control (*Figure 2C*). On the other hand, HG enhanced the effect of H_2O_2 (b4 *vs.* b2), as shown in *Figure 2D* (P<0.05).

The expression of $p21^{Waf1}$ protein in the HG group (a3) was maximal, followed by the a2, a6, a8, a1, a4, a5, and a7 groups (*Figure 2E*). As a response to HG stimulation, $p21^{Waf1}$ protein expression was higher in HPMCs than in controls in a dose-dependent manner (a3 *vs.* a2, a2 *vs.* a1, P<0.05). This effect was reduced significantly by the antioxidant (a6 *vs.* a3, P<0.05). No difference was observed between *p21* expression in the high osmolality (a4) group and the control group (*Figure 2E*). The expression of $p21^{Waf1}$ protein in the HG group (b3) was the strongest, followed by the b4, b5, b1, b2, and b6 groups. We found that exogenous H_2O_2 elevated the expression of *p21* (b1 *vs.* b6, b1 *vs.* b2, P<0.05), which was enhanced by HG (b3 *vs.* b1), and the antioxidant counteracted the effect of exogenous H_2O_2 (b3 *vs.* b5, P<0.05) (*Figure 2F*). The representative ICC images for *p21* are shown in *Figure 2G*.

The results of Western blot were similar to that of ICC. The expression between the HG group (a3) and the HG plus H_2O_2 group (b3) did not differ significantly, and both groups had stronger expression than the control group (a1). The expression (a6) was reduced after the addition of antioxidants but remained higher than the control (P<0.05) (*Figure 2H*).

Effects of various stimulations on $p27^{Kip1}$ expression

The representative results of RT-PCR for *p27* are shown in *Figure 3A,3B*. Following stimulation of HPMCs with HG (*Figure 3A*) and H_2O_2 (*Figure 3B*), no significant differences were observed in *p27* gene expression (*Figure 3A,3B*) (P>0.05).

Following the stimulation of HPMCs with HG, the expression of $p27^{Kip1}$ protein in the a3, a6, a8, and a2 groups was similar, with approximately 100% positive expression and no significant differences. Moreover, *p27* expression in the a1, a4, a5, and a7 groups was also similar, approximately 75% positive, which was significantly different when compared to that of the a3, a6, a8, a2 groups (P<0.05). This indicated that HG increased *p27* expression. However, a significant change was observed in *p27* expression after pyruvate addition. Also, no difference was observed in *p27* expression between the high osmolality group (a4) and the control group (*Figure 3C*). Both exogenous H_2O_2 and H_2O_2 plus glucose elevated the expression of *p27*. The positive cell percent of all 5 groups with HG or H_2O_2 was nearly 100% compared to that of the b6 group (75%), which reached statistical significance (*Figure 3D*). The representative ICC images for *p27* are shown in *Figure 3E*. The results of Western blot were similar to $p21^{Waf1}$ (*Figures 2H,3F*).

Discussion

In our study, we preliminarily demonstrated: (I) the effect of ROS and HG on the growth (proliferation) of HPMCs and the role of *p21* and *p27* in this process; (II) the role of ROS in HG-induced changes in cell growth in HPMCs.

Effects of HG and exogenous H_2O_2 on the growth and cell cycle of HPMCs

This study suggested that HG inhibits cell proliferation, as described previously (4). We also found that exogenous H_2O_2 inhibits the proliferation of HPMCs in a dose-dependent manner. The low concentration of H_2O_2 did not have an obvious effect, which is supported by similar study on cultured human tracheal epithelium and renal proximal tubule cells (3). On the other hand, we also observed that the addition of H_2O_2 in HG medium enhanced the cytotoxicity of H_2O_2. These results suggest that peritonitis or long-term dialysis might cause injury to CAPD patients from the increased generation of H_2O_2, which might be harmful in the presence of HG.

We speculated that these effects are related to the changes in HG- or exogenous H_2O_2-induced cell cycle. In this study, we found that both HG and exogenous H_2O_2 can induce cell cycle arrest of HPMCs at the G_1 phase, but not with HG-induced high osmolality. This finding was supported by Zhang *et al.* (10) who demonstrated that

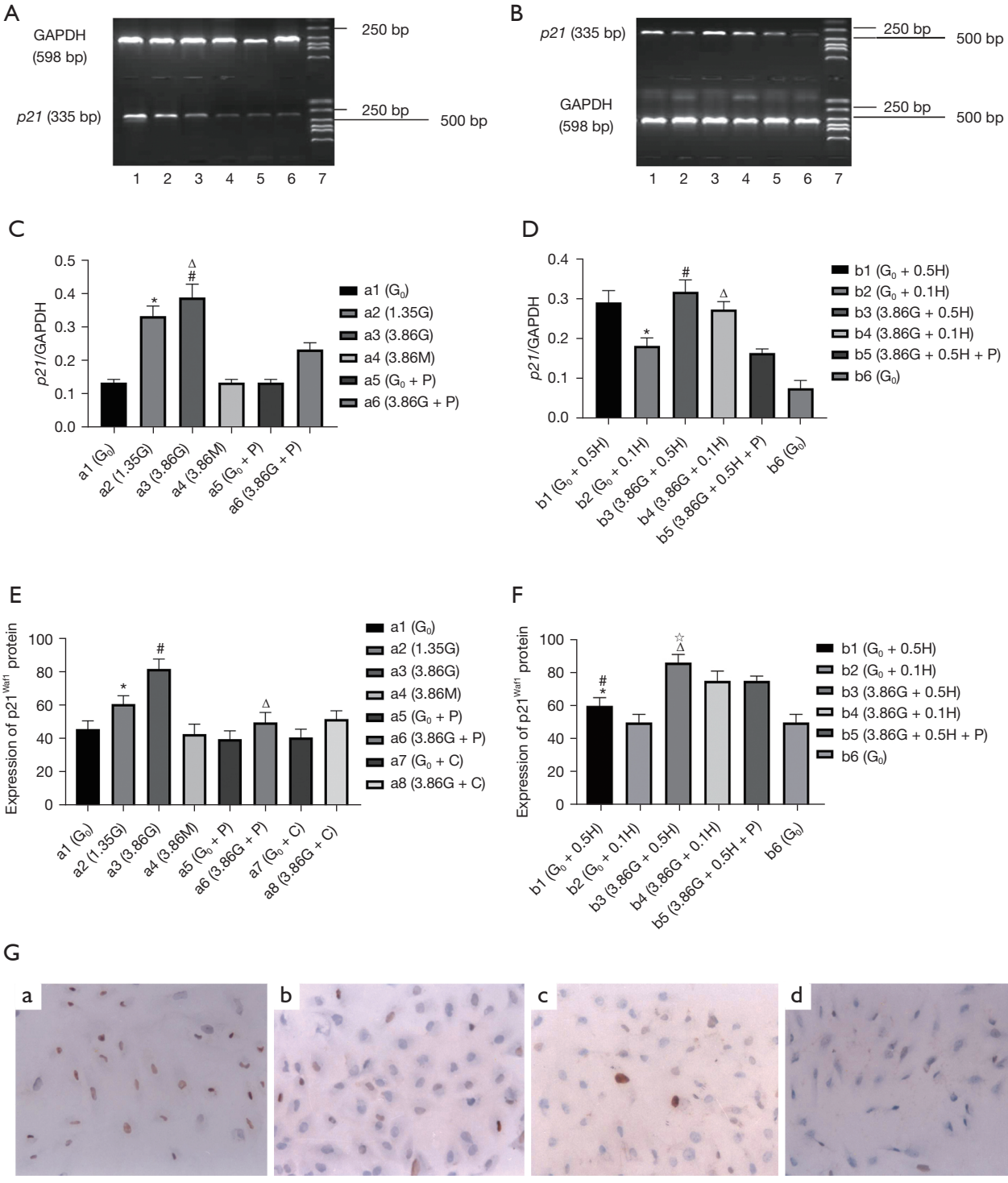

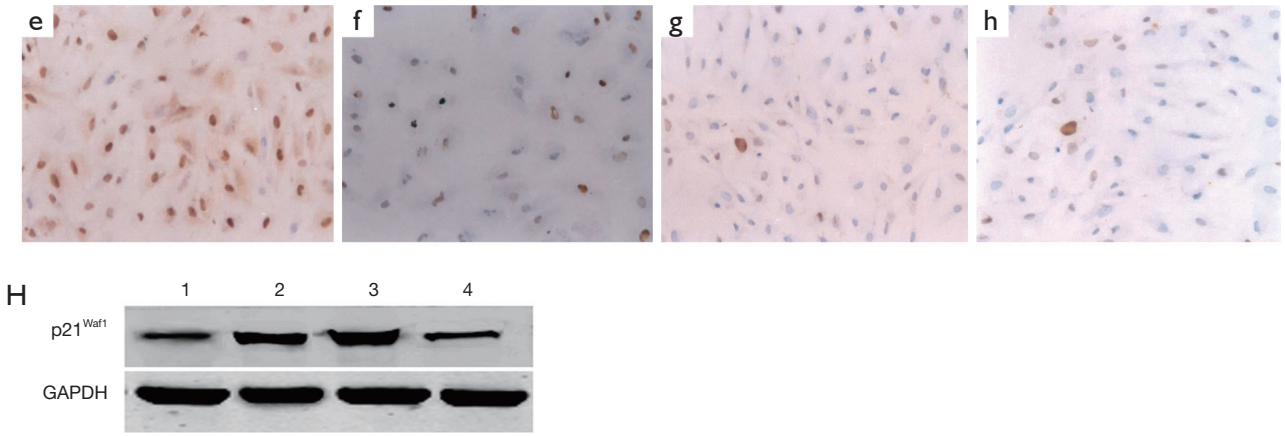

Figure 2 Effects of various stimulations on *p21*^{Waf1}. (A,C) Effect of glucose, mannitol, and pyruvate on the expression of *p21*^{Waf1} mRNA in HPMCs. Lane 1: a3 (3.86G); lane 2: a2 (1.38G); lane 3: a6 (3.86G + P); lane 4: a1 (G_0); lane 5: a4 (3.86M); lane 6: a5 (G_0 + P); lane 7: marker. *, a2 *vs.* a1, P<0.05; #, a3 *vs.* a2, P<0.05; △, a3 *vs.* a6, P<0.05. (B,D) The effect of glucose, H_2O_2, and pyruvate on the expression of *p21*^{Waf1} mRNA in HPMCs. Lane 1: b1 (G_0 + 0.5H); lane 2: b2 (G_0 + 0.1); lane 3: b3 (3.86G + 0.5H); lane 4: b4 (3.86G + 0.1H); lane 5: b5 (3.86G + 0.5H + P); lane 6: b6 (G_0); lane 7: marker. *, b2 *vs.* b6, P<0.05; #, b3 *vs.* b5, P<0.05; △, b4 *vs.* b2, P<0.05. (E-G) ICC analysis. (E) Effect of glucose and antioxidants on the expression of p21^{Waf1} protein. *, a2 *vs.* a1, P<0.05; #, a3 *vs.* a2, P<0.05; △, a6 *vs.* a3, P<0.05. (F) Effect of glucose, H_2O_2, and pyruvate (antioxidant) on the expression of p21^{Waf1} protein. *, b1 *vs.* b2, P<0.05; #, b1 *vs.* b6, P<0.05; △, b3 *vs.* b1, P<0.05; ☆, b3 *vs.* b5, P<0.05. (G) ICC analysis of the expression of p21^{Waf1} protein with glucose, H_2O_2, and pyruvate (antioxidant) in HPMCs (×20) (DAB staining). a, a3 (3.86G); b, a2 (1.35G); c, a6 (3.86G + P); d, a1 (G_0); e, b3 (3.86G + 0.5H); f, b5 (3.86G + 0.5H + P); g, b1 (G_0 + 0.5H); h, b6 (G_0). (H) Western blot analysis of p21^{Waf1} protein expression in the HPMCs of each group. Lane 1: G_0 (a1); lane 2: 3.86G (a3); lane 3: 3.86G + 0.5H (b3); lane 4: 3.86G + P (a6). a1: with 0.1% glucose in DMEM (G_0), as the control group; a2: with 1.35% glucose (1.35G); a3: with 3.86% glucose (3.86G). a4: with 3.86% mannitol (3.86M); a5: with pyruvate 35 mmol/L in DMEM (G_0 + P); a6: with 3.86% glucose and pyruvate 35 mmol/L (3.86G + P); a7: with catalase 500 U/L (G_0 + C); a8: with 3.86% glucose and catalase 500 U/L in DMEM (3.86G + C). b1: with H_2O_2 0.5 mmol/L in DMEM (G_0 + 0.5H); b2: with H_2O_2 0.1 mmol/L (G_0 + 0.1H); b3: with H_2O_2 0.5 mmol/L and 3.86% glucose (3.86G + 0.5H); b4: with H_2O_2 0.1 mmol/L and 3.86% glucose (3.86G + 0.1H); b5: with H_2O_2 0.5 mmol/L, 3.86% glucose, and pyruvate 35 mmol/L (3.86G + 0.5H + P); b6: with 0.1% glucose (G_0), as the control group. HPMCs, human peritoneal mesothelial cells; H_2O_2, hydrogen peroxide; ICC, immunocytochemistry; DAB, 3,3'-diaminobenzidine; DMEM, Dulbecco's modified Eagle's medium.

H_2O_2 induced the premature senescence of human diploid fibroblasts by increasing *p21* gene expression and arresting the cell cycle at the G_1 phase. Therefore, based on the current results, we can deduce that HG inhibits the growth of HPMCs by arresting cell cycle progression.

Effects of HG and exogenous H_2O_2 on the expression of p21^{Waf1} and p27^{Kip1} in HPMCs

In diabetes research, *p21* and *p27* have been associated with the cytotoxicity of HG. We found that both HG and exogenous H_2O_2 increased the expression of *p21*^{Waf1}, which was supported by Lin *et al.* (8) in a diabetic nephropathy study and Kim *et al.* (11) in human fibroblast cells. For p27^{Kip1}, protein expression was increased by either HG or exogenous H_2O_2, but neither of them influenced the gene expression of *p27*^{Kip1}. Elson *et al.* (13) demonstrated that in most situations, the gene expression of *p27* is consistent in the cell cycle, indicating that the alteration of *p27* occurs at the protein level, corresponding to our results. In a study on diabetic nephropathy, Aitken *et al.* (14) demonstrated that HG inhibits cell proliferation (cell growth) in a dose-dependent manner, which is associated with the increased expression of *p27*^{Kip1}. Thus, we inferred that both HG and exogenous H_2O_2 can inhibit the growth of HPMCs by arresting cell cycle progression via increased expression of *p21* and *p27*.

Effects of endogenous ROS on HG-induced growth inhibition and the expression of p21^{Waf1} and p27^{Kip1} in HPMCs

HG-induced growth inhibition and cell cycle arrest in

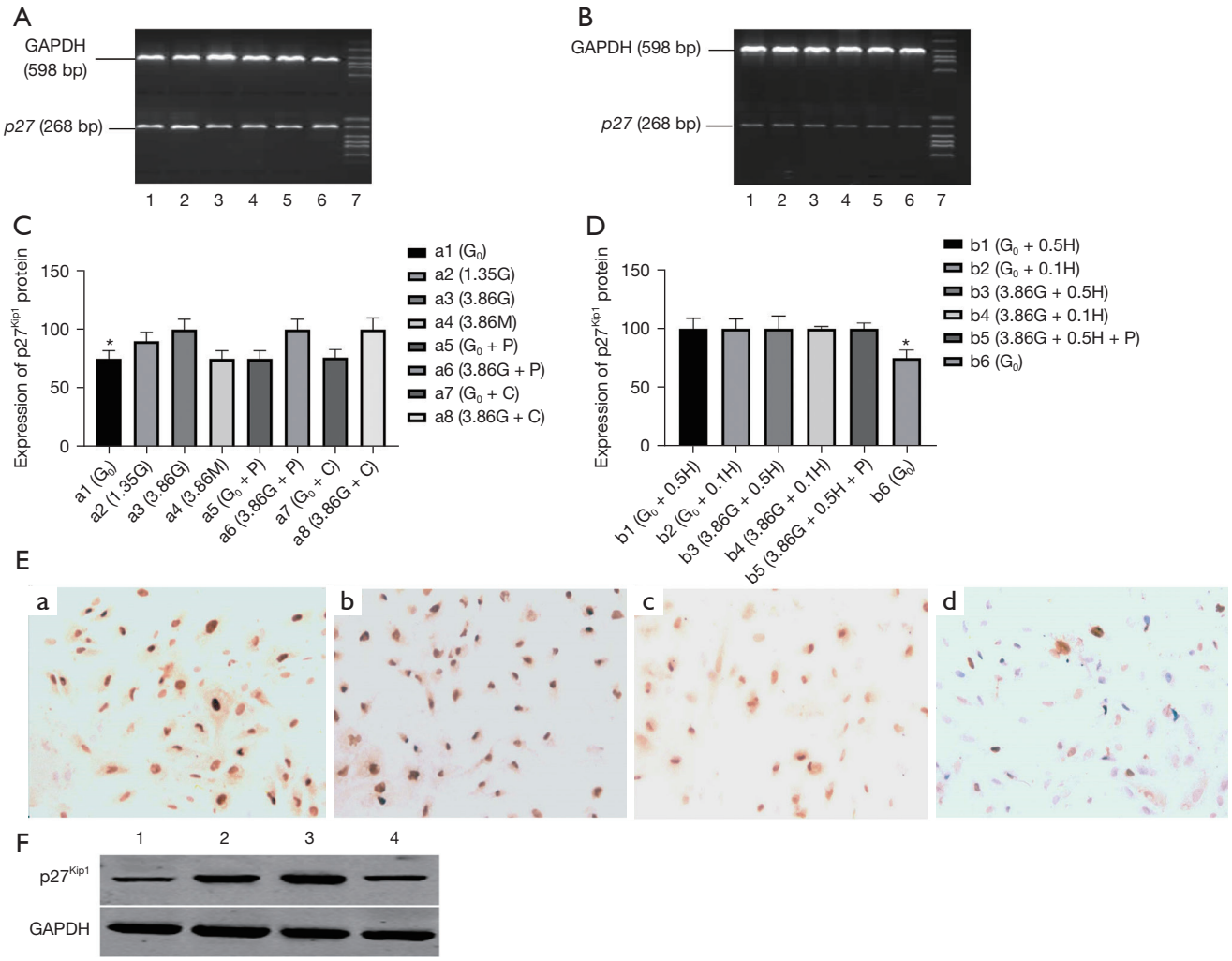

Figure 3 Effects of various stimulations on *p27*^{Kip1}. (A) Effect of glucose, mannitol, and pyruvate on the expression of *p27*^{Kip1} mRNA in HPMCs. No significant differences were detected in *p27* gene expression (P>0.05). Lane 1: a3 (3.86G); lane 2: a2 (1.38G); lane 3: a6 (3.86G + P); lane 4: a1 (G_0); lane 5: a4 (3.86M); lane 6: a5 (G_0 + P); lane 7: marker. (B) Effect of glucose, H_2O_2, and pyruvate on the expression of *p27*^{Kip1} mRNA in HPMCs. No significant differences were detected in *p27* gene expression (P>0.05). Lane 1: b1 (G_0 + 0.5H); lane 2: b2 (G_0 + 0.1H); lane 3: b3 (3.86G + 0.5H); lane 4: b4 (3.86G + 0.1H); lane 5: b5 (3.86G + 0.5H + P); lane 6: b6 (G_0); lane 7: marker. (C-E) ICC analysis. (C) Effect of glucose and antioxidants on the expression of p27^{Kip1} protein. *, a1 *vs.* a2, a1 *vs.* a3, P<0.05. (D) Effect of glucose, H_2O_2, and antioxidants on the expression of p27^{Kip1} protein. *, b6 *vs.* b1, P<0.05. (E) ICC analysis of the expression of p27^{Kip1} protein with glucose, H_2O_2, and pyruvate (antioxidant) in HPMCs (×20) (DAB staining). a, a3 (3.86G); b, a6 (3.86G + P); c, b1 (G_0 + 0.5H); d, a1 (G_0). (F) Western blot analysis of p27^{Kip1} protein expression in HPMCs in each group. Lane 1: G_0 (a1); lane 2: 3.86G (a3); lane 3: 3.86G + 0.5H (b3); lane 4: 3.86G + P (a6). a1: with 0.1% glucose in DMEM (G_0), as the control group; a2: with 1.35% glucose (1.35G); a3: with 3.86% glucose (3.86G). a4: with 3.86% mannitol (3.86M); a5: with pyruvate 35 mmol/L in DMEM (G_0 + P); a6: with 3.86% glucose and pyruvate 35 mmol/L (3.86G + P); a7: with catalase 500 U/L (G_0 + C); a8: with 3.86% glucose and catalase 500 U/L in DMEM (3.86G + C). b1: with H_2O_2 0.5 mmol/L in DMEM (G_0 + 0.5H); b2: with H_2O_2 0.1 mmol/L (G_0 + 0.1H); b3: with H_2O_2 0.5 mmol/L and 3.86% glucose (3.86G + 0.5H); b4: with H_2O_2 0.1 mmol/L and 3.86% glucose (3.86G + 0.1H); b5: with H_2O_2 0.5 mmol/L, 3.86% glucose, and pyruvate 35 mmol/L (3.86G + 0.5H + P); b6: with 0.1% glucose (G_0), as the control group. HPMCs, human peritoneal mesothelial cells; H_2O_2, hydrogen peroxide; ICC, immunocytochemistry; DAB, 3,3'-diaminobenzidine; DMEM, Dulbecco's modified Eagle's medium.

HPMCs are attributed to a complex mechanism. Recently, the role of ROS in PD has been under intense focus. ROS are now being accepted as signaling molecules which activate protein kinases, transcription factors, and gene expression (15). Horiuchi *et al.* (16) found that cultured HPMCs can produce H_2O_2. Moreover, mesothelial cells in culture significantly increased the generation of H_2O_2 when exposed to HG. Recently, a study measured ROS generation by HPMCs cultured under HG using a ROS-sensitive fluorescence probe and confocal microscope (15). On the other hand, peritoneal infection or long-term, continuous stimulation by the biologically incompatible peritoneal dialysate is likely to produce ROS in the peritoneal cavity, which might harm HPMCs and CAPD patients.

In this study, HG-induced $p21^{Waf1}$ expression was downregulated at both the gene and protein level after the addition of antioxidants to the HG media. Moreover, G_1 phase arrest and inhibited cell growth were attenuated, indicating that the antioxidants (pyruvate and catalase) counteracted the effect of endogenous ROS. Shostak *et al.* reported that pyruvate could improve the peritoneal dialysate-induced inhibition of proliferation in HPMCs (17). These results were supported by other similar study (18). We also found a specific scavenger for H_2O_2, namely catalase, which can improve the inhibition of cell growth. This finding suggests endogenous H_2O_2 is a vital part of ROS, which is linked to HG-induced cell growth inhibition. Although a study has reported the ROS-increased expression of $p27^{Kip1}$ and HG-increased expression of $p27^{Kip1}$, the effect of endogenous ROS is not certain. At least, in our preliminary study, we could not demonstrate any significant influence of endogenous ROS on the expression of *p27*, as shown by ICC results in our previous study (19). Thus, we infer that in our methods, the incubation time of HG with HPMCs is limited, which might restrict the effect of ROS. Therefore, we could not detect the effect of endogenous H_2O_2 on *p27* expression with ICC, which is different from CAPD *in vivo*. Also, the HPMCs were in contact with HG for a prolonged period. Western blotting presented a different positive result, indicating a certain effect of endogenous ROS on *p27* expression. These discrepancies in the results may be due to the high sensitivity of Western blots compared to ICC in quantitative analysis. Thus, it may be inferred that HG-dependent cell damage is a function of both the reduced production of scavengers and the increased generation of ROS by mesothelial cells.

Interestingly, one study suggested that HG increases the expression of *p21* and *p27*, mediated by *TGF-β1* (20). These results indicate that chronic exposure to elevated glucose might result in TGF-β1-mediated accelerated senescence of HPMCs *in vitro*. Jin *et al.* demonstrated that the role of HG is related to ROS (21), but to the best of our knowledge, the role of ROS in *p21* and *p27* expression in HPMCs has not yet been studied. Our preliminary results suggested that HG inhibits cell growth by increasing ROS-mediated *p21* and *p27* expression.

Nevertheless, the present study has some limitations. We could not directly measure H_2O_2 concentration in HG medium. Furthermore, the significance of direct measurement is with little meaning since the effect of H_2O_2 could be influenced by other factors, such as cell types and the microenvironment. Our previous study found that high glucose increased the expression of monocyte chemoattractant protein-l (MCP-1) and interlukin-8 (IL-8), and endogenous ROS could induce the expression of *IL-8* (22). Many researches have confirmed that the classical signaling pathway involved about $p21^{Waf1}$ is $p21^{WAF1}$/*CIP1*, and the classical signaling pathway involved in $p27^{Kip1}$ is mitogen-activated extracellular signal-regulated kinase-extracellular regulated protein kinases (*MEK-ERK*) signaling (23,24). But the mechanisms of HG-induced changes in the cell cycle and cell proliferation in HPMCs have not yet been clarified, although ROS may play a role. Thus, the signal transduction pathways through which ROS affects the cell cycle and proliferation need to be investigated further.

Acknowledgments

We thank Prof. Yijie Wu, Department of Endocrinology, Shanghai General Hospital, for revising the English manuscript; Prof. Shanlin Liu, Department of Biochemistry, Shanghai Medical College, Fudan University, China, for his kind suggestions in this study; and Dr. Kaitlyn Reasoner for her kind help in revising and polishing the English writing of this article.

Funding: This study was supported by the National Natural Science Foundation of China (No. 81800676).

Footnote

Reporting Checklist: The authors have completed the MDAR reporting checklist. Available at https://atm.amegroups.com/article/view/10.21037/atm-22-4352/rc

Data Sharing Statement: Available at https://atm.amegroups.com/article/view/10.21037/atm-22-4352/dss

Conflicts of Interest: All authors have completed the ICMJE uniform disclosure form (available at https://atm.amegroups.com/article/view/10.21037/atm-22-4352/coif). The authors have no conflicts of interest to declare.

Ethical Statement: The authors are accountable for all aspects of the work in ensuring that questions related to the accuracy or integrity of any part of the work are appropriately investigated and resolved.

References

1. Zhu N, Gu L, Jia J, et al. Endothelin-1 triggers human peritoneal mesothelial cells' proliferation via ERK1/2-Ets-1 signaling pathway and contributes to endothelial cell angiogenesis. J Cell Biochem 2019;120:3539-46.
2. Margetts PJ. Twist: a new player in the epithelial-mesenchymal transition of the peritoneal mesothelial cells. Nephrol Dial Transplant 2012;27:3978-81.
3. Shen S, Ji C, Wei K. Cellular Senescence and Regulated Cell Death of Tubular Epithelial Cells in Diabetic Kidney Disease. Front Endocrinol (Lausanne) 2022;13:924299.
4. Zhang Y, Xiao WH, Huang YX, et al. MiR-128-3p inhibits high-glucose-induced peritoneal mesothelial cells fibrosis via PAK2/SyK/TGF-β1 axis. Ther Apher Dial 2022. [Epub ahead of print]. doi: 10.1111/1744-9987.13912.
5. Krediet RT. Acquired Decline in Ultrafiltration in Peritoneal Dialysis: The Role of Glucose. J Am Soc Nephrol 2021;32:2408-15.
6. Zhu N, Wang L, Guo H, et al. Thalidomide Suppresses Angiogenesis Through the Signal Transducer and Activator of Transcription 3/SP4 Signaling Pathway in the Peritoneal Membrane. Front Physiol 2021;12:712147.
7. Roumeliotis S, Dounousi E, Salmas M, et al. Unfavorable Effects of Peritoneal Dialysis Solutions on the Peritoneal Membrane: The Role of Oxidative Stress. Biomolecules 2020;10:768.
8. Lin SH, Ho WT, Wang YT, et al. Histone methyltransferase Suv39h1 attenuates high glucose-induced fibronectin and p21(WAF1) in mesangial cells. Int J Biochem Cell Biol 2016;78:96-105.
9. Chidawanyika T, Supattapone S. Hydrogen Peroxide-induced Cell Death in Mammalian Cells. J Cell Signal 2021;2:206-11.
10. Zhang SL, Li BL, Li W, et al. Retracted: The Effects of Ludartin on Cell Proliferation, Cell Migration, Cell Cycle Arrest and Apoptosis Are Associated with Upregulation of p21WAF1 in Saos-2 Osteosarcoma Cells In Vitro. Med Sci Monit 2021;27:e931590.
11. Kim W, Kwon HJ, Jung HY, et al. P27 Protects Neurons from Ischemic Damage by Suppressing Oxidative Stress and Increasing Autophagy in the Hippocampus. Int J Mol Sci 2020;21:9496.
12. Zhang J, Buranjiang G, Mutalifu Z, et al. KIF14 affects cell cycle arrest and cell viability in cervical cancer by regulating the p27Kip1 pathway. World J Surg Oncol 2022;20:125.
13. Elson DJ, Nguyen BD, Wood R, et al. The cyclin-dependent kinase inhibitor p27Kip1 interacts with the aryl hydrocarbon receptor and negatively regulates its transcriptional activity. FEBS Lett 2022;596:2056-71.
14. Aitken TJ, Crabtree JE, Jensen DM, et al. Decreased proliferation of aged rat beta cells corresponds with enhanced expression of the cell cycle inhibitor p27KIP1. Biol Cell 2021;113:507-21.
15. Jia M, Qiu H, Lin L, et al. Inhibition of PI3K/AKT/mTOR Signalling Pathway Activates Autophagy and Suppresses Peritoneal Fibrosis in the Process of Peritoneal Dialysis. Front Physiol 2022;13:778479.
16. Horiuchi T, Matsunaga K, Banno M, et al. HPMCs induce greater intercellular delocalization of tight junction-associated proteins due to a higher susceptibility to H2O2 compared with HUVECs. Perit Dial Int 2009;29:217-26.
17. Shostak A, Gotloib L, Kushnier R, et al. Protective effect of pyruvate upon cultured mesothelial cells exposed to 2 mM hydrogen peroxide. Nephron 2000;84:362-6.
18. Zhang JJ, Shen HQ, Deng JT, et al. Effect of peritoneal dialysis solution with different pyruvate concentrations on intestinal injury. Exp Biol Med (Maywood) 2020;245:644-53.
19. Tang ZH, Yao J, Liu J, et al. Reactive oxygen species and high glucose induce growth inhibition of human peritoneal mesothelial cells through arresting cell cycles progression.

Chinese Journal of Nephrology 2003;19:223-7.
20. Ksiazek K, Korybalska K, Jörres A, et al. Accelerated senescence of human peritoneal mesothelial cells exposed to high glucose: the role of TGF-beta1. Lab Invest 2007;87:345-56.
21. Jin QH, Hu XJ, Zhao HY. Curcumin activates autophagy and attenuates high glucose-induced apoptosis in HUVECs through the ROS/NF-κB signaling pathway. Exp Ther Med 2022;24:596.
22. Tang ZH, Zhang Z, Liu J, et al. Effect of high glucose on the expression of IL-8 and MCP-1 in human peritoneal mesothelial cells and the role of reactive oxygen species in this course. Chinese Journal of Blood Purification 2002;1:12-5.
23. Cheng SY, Seo J, Huang BT, et al. Mitomycin C and decarbamoyl mitomycin C induce p53-independent p21WAF1/CIP1 activation. Int J Oncol 2016;49:1815-24.
24. Bhatt KV, Spofford LS, Aram G, et al. Adhesion control of cyclin D1 and p27Kip1 levels is deregulated in melanoma cells through BRAF-MEK-ERK signaling. Oncogene 2005;24:3459-71.

(English Language Editor: C. Betlazar-Maseh)

Cite this article as: Zhu N, Tang Y, Yuan W, Tang Z. Role of reactive oxygen species in high concentration glucose-induced growth inhibition of human peritoneal mesothelial cells. Ann Transl Med 2022;10(19):1065. doi: 10.21037/atm-22-4352

